ISSN 1061-9348, Journal of Analytical Chemistry, 2017, Vol. 72, No. 4, pp. 445–459. © Pleiades Publishing, Ltd., 2017.

ARTICLES

Lactose Tailored Boronic Acid Conjugated Fluorescent Gold Nanoclusters for Turn-on Sensing of Dopamine[1]

J. S. Anjali Devi, B. Aswathy, Sasidharan Asha, and Sony George*

University of Kerala, Department of Chemistry, Kariavattom Campus 695581, India

**e-mail: emailtosony@gmail.com*

Received July 10, 2015; in final form, August 31, 2016

Abstract—Dopamine being a neurotransmitter and chemical messenger plays a vivacious role in a number of significant medical conditions like Parkinson's disease, Attention Deficit Hyperactivity Disorder, Schizophrenia, and drug addiction. As turn-on sensors have a superior level of selectivity than fluorescence quenching based sensors, we developed a fluorescence retrieval strategy for dopamine sensing. Here, highly fluorescent amino phenyl boronic acid (**APBA**)–conjugated gold nanocluster (**Au–BSA–APBA** probe) has been synthesised from bovine serum albumin–protected gold nanocluster (**Au–BSA NCs**). Boronic acid forms boronate ester with disaccharides such as lactose due to its affinity to polyols. Hence fluorescence of Au–BSA–APBA probe is quenched when it binds with lactose molecules through boronate ester formation. The fluorescence of Au–BSA–APBA–lactose system can be retrieved (turn-on) with dopamine by the competitive displacement of lactose from the probe surface which suggests the higher affinity of boronic acid to the catechol group of dopamine. Furthermore, real samples spiked with dopamine including human serum and urine were analysed using this turn-on sensor and showed excellent recovery percentage. The developed fluorescent sensor offered high selectivity for dopamine over other catecholamines and aminoacids with detection limit as low as 0.7 μM.

Keywords: fluorescent gold nanocluster, boronic acid, turn-on sensing, dopamine

DOI: 10.1134/S1061934817040037

The desire to analyse biological systems with environmentally friendly and biocompatible sensors have driven biosensor research attention towards gold nanoclusters (**AuNCs**) which emerge as an auspicious substitute for toxic quantum dots and organic dyes. The extremely small gold nanoparticles (≤2 nm) with size comparable to the Fermi wavelength of electron in the conduction band of gold (ca. 0.7 nm) exhibit separate electronic energy levels and are generally termed gold nanoclusters [1–5]. These artificial atomic clusters, by virtue of their intermittent energy levels show molecule-like properties such as photoluminescence, chirality, magnetism and localised charge, are considered to be the missing link between atomic gold and gold nanoparticles [3, 4, 6]. The size-dependent fluorescence of molecule-like AuNCs originates from LUMO–HOMO electronic transition from the valence band (filled $5d^{10}$) to the conduction band ($6sp^1$) [7] and falls on visible to Near Infrared (**NIR**) region of electromagnetic spectrum [6].

In spite of these intriguing features, synthesis of AuNCs is a challenging process owing to limited control over size distribution as well as ultra-small size regime. The nucleation through the reduction of a gold salt ($HAuCl_4$) with a weak reducing agent such as glutathione [8], phenyl ethyl thiolate [3], dodecanethiol [9], DNA [10, 11], phosphonium salt [9], dendrimer [12], aminoacids [7, 13, 14], proteins [4, 15–17] in the presence of a capping agent is the principle behind the 'bottom-up synthesis' of AuNCs [9]. As said, AuNCs by virtue of their blessed properties like biocompatibility, photo-stability, tunable fluorescence spanning from visible to NIR region, good quantum yield and large Stokes shift are considered 'appropriate candidates' for bioprobe synthesis. These AuNCs built bioprobes are employed in sensing [7, 8, 11, 13, 15, 18–27], immunoassays [10, 28] and imaging [9, 16, 29–31], as photocatalysts [32], contrast agents [33] and biomarkers [34–36]. To meet the challenges in preparing biocompatible AuNCs with constant size distribution, a protein (BSA)-directed green synthesis of homogeneous near IR fluorescent Au–BSA NCs at pH~12 has been proposed in 2009 [4] which finds application in sensing of target species like Cu^{2+} [24, 25], trypsin [37], Hg^{2+} [22], biological thiols [19] and quercetin [38]. These literature reports driven us to the conclusion that NIR fluorescence emission of Au–BSA NCs is efficient enough to act as a transducer component in our proposed biosensor.

[1] The article is published in the original.

Table 1. Analytical performances of other reported methods for dopamine sensing

Sensor system	Mechanism	Response mode	Selectivity	Limit of detection	Reference
Chromatography					
HPLC–MS	–	Mass spectrum	Interference from CA[a]; no intereference to AA[b] and UA[c]	6.5 ng/mL	[48]
Electroanalytical method					
Carbon electrode	Oxidation	Voltammetry	Interference from AA; no intereference to CA and UA	90 nM	[45]
Screen printed graphene electrode	Oxidation	Voltammetry	Interference from AA and UA; no intereference to CA	0.12 μM	[46]
Gold electrode	Oxidation	Voltammetry	No interference from UA; no interference to AA and CA	20 nM	[47]
Fluorescent method					
CdSe nanocrystals	Photoelectron transfer	Turn-off			[49]
Gold nanocluster	Boronate ester formation	Turn-on	No interference from AA, UA and CA	0.7 μM	Present work

[a]CA, other catecholamines; [b]AA, ascorbic acid; [c]UA, uric acid.

A relevant area of biosensor where researchers contribute their time and money is that of saccharide sensing. The saccharide sensing in lower concentration range has great application in determination of food quality and clinical diagnostics. For instance, detection of lactose in milk is significant as its concentration determines the properties of milk. One of the methods to detect lactose in milk involves enzymatic hydrolysis of lactose which is a time-consuming complex process. Alternatively, the estimation of lactose in milk using standard HPLC with corona charged aerosol detection has been reported. These techniques are not so environmentally friendly as they use several hazardous reagents.

In this problematic scenario of unfriendly reagents and time-consuming procedures for saccharide recognition, boronic acids emerged as a green alternative owing to its ultimate degradation to non-toxic boric acids [39]. This movement in sensor research can be evidenced from tremendous scientific reports published in recent years regarding the fabrication of boronic acid–functionalised inorganic nanoparticles for sensing and quantification of saccharides [40–42]. For instance, a-multifunctional Fe_3O_4@Au nanofibres have been prepared for glycoprotein imprinting [42]. But no reports regarding saccharide sensing using boronic acid conjugated AuNCs has been found to the best of our knowledge. In this context, we felt that the interaction of boronic acid with 1,2-*cis*-diol is an intriguing recognition platform not only for saccharides but also for catechol amines like dopamine.

Dopamine is a catechol amine which functions as a neurotransmitter. It has a vital role in brain functioning. Brain disorders like schizophrenia, Parkinson's disease, attention deficit hyperactivity disorder, and drug addiction involves altered level of dopamine activity [43, 44]. Outside the nervous system, dopamine works as a chemical messenger. Further, this prospective biomolecule is extensively used as a potential drug in the form of injection for the treatment of severe hypotension or cardiac arrest. Therefore, sensing of this catechol amine has a wide range of application in therapeutics and medical diagnosis. A major part of research concerning dopamine determination is concentrated on development of myriad electrochemical sensors working on the catalytic oxidation of dopamine [45–47] (Table 1). Unfortunately, these electrochemical sensors are unable to completely solve the problem of interferences from coexisting ascorbic acid and uric acid. Likewise, the chromatographic techniques for dopamine determination [48] cannot be an appealing substitute for electroanalytical methods as these techniques required complicated time-consuming expensive procedures, specific operating skills and specialised equipment. Although fluorescent sensors are associated with high grade of selectivity, sensitivity and simplicity, they were not so exploited in dopamine detection. However, spectroscopic methods for dopamine detection like sensors containing CdSe nanocrystals with decent detection limits has been reported in this scenario in which analysis is based on the quenching of fluorescence [49]. But then again the use of toxic chemicals like Cd or Se is not a desirable approach for biosensor while considering environmental safety and human health. Moreover, fluorescent turn-on sensor is preferable over analogous turn-off sensors since it is comparatively easy to detect evolving bright signal in dark back ground rather than diminishing of already existing bright signal [50]. Consequently, turn-on sensing has

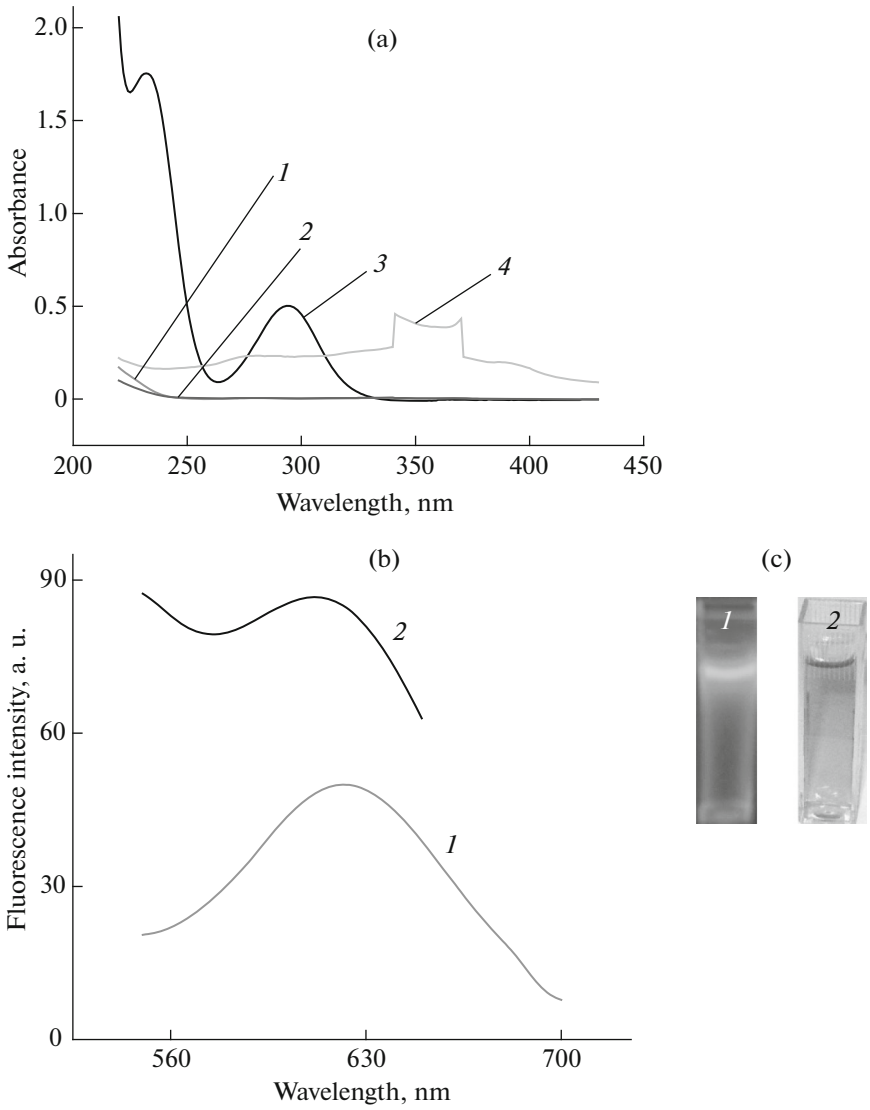

Fig. 1. (a) UV-visible absorption spectra of alkaline solution of BSA protein (*1*); gold nanoclusters prepared using BSA directed synthesis (*2*); solution of aminophenyl boronic acid alone (*3*); boronic acid conjugated gold nanoclusters (*4*). (b) Fluorescence spectra of gold nanoclusters (Au–BSA NCs) (*1*); boronic acid conjugated gold nanoclusters (Au–BSA–APBA probe) (*2*). Excitation wavelength: 480 nm. (c) The photographs of Au–BSA NCs under UV irradiation (*1*) and under visible light (*2*).

driven much research interest in recent years [50, 51]. Thus, sensing strategy based on retrieval of fluorescence has a greater level of selectivity and feasible detection of signal than quenching based sensing and will be a boon to the determination of dopamine. In this context, it has become interesting to design an 'environmentally friendly' and simple fluorimetric turn-on assay for dopamine.

In this work we are presenting a fluorescent probe (Au–BSA–APBA) in which the fluorescence can be switched off by lactose (turn-off) followed by the selective retrieval of fluorescence with dopamine (turn-on).

EXPERIMENTAL

Reagents and materials. Gold chloride was purchased from Oxford Laboratory (Mumbai, India). Bovine serum albumin (BSA, fraction V) was from Merck Specialities Private Ltd. (Mumbai, India). 3-Aminobenzene boronic acid monohydrate and dopamine hydrochloride were obtained from Alfa Aesar (Heysham, England). Lactose monohydrate, Sodium Hydroxide pellets, Adrenaline, and Noradrenaline were bought from Central Drug House (New Delhi, India). 1-Ethyl-3-(3-dimethyl aminopropyl)carbodiimide (**EDC**), N-hyroxysuccinimide (**NHS**), L-histidine, L-arginine and L-lysine monohydrchloride were purchased from Sisco Research

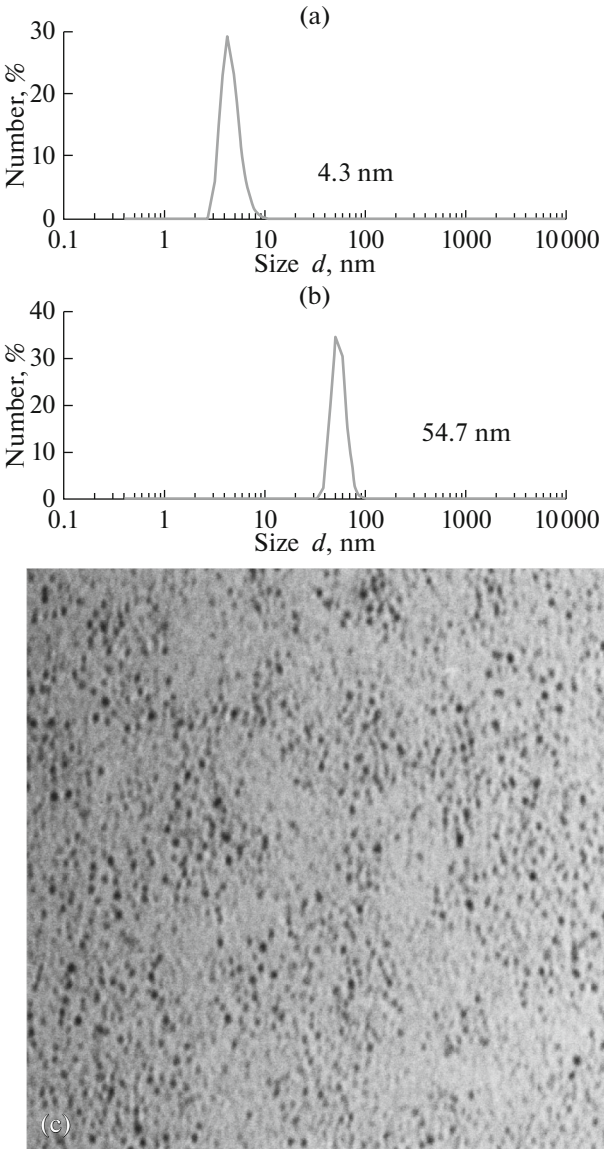

Fig. 2. (a) DLS plot of gold nanoclusters (Au–BSA NCs); the size was recorded as 4.3 nm. (b) The DLS plot of lactose tailored boronic acid conjugated gold nanoclusters (Au–BSA–APBA–lactose conjugate); the size was recorded as 54.7 nm. (c) TEM image of Au–BSA NCs.

Laboratories Pvt. Ltd. (Mumbai, India). D-Glucose (anhydrous), L-ascorbic acid and uric acid were obtained from Spectrum Reagents and Chemicals Pvt. Ltd. (Cochin, India). All glass wares were thoroughly cleaned with aqua regia ($HCl : HNO_3 = 3 : 1$), rinsed with distilled water and then dried in an air oven prior to use. All reagents were of analytical-reagent grade and used without purification or treatment.

Apparatus. Absorbance spectra were recorded using Jasco V-550 UV-Vis spectrophotometer. The samples were analysed in a quartz cuvette with a path length of 1 cm. Fluorescence spectra were recorded using a Jasco FP-750 fluorescence spectrophotometer. The size distribution of particles was analysed using DLS equipment Delsa Nano S Particle Analyser of Beckman Coulter Company. Transmission electron microscopy (**TEM**) measurements were taken with a JEOL 200 CH TEM. Fourier transform infrared (**FT-IR**) spectra were recorded using the Brucker alpha T-series FT-IR spectrophotometer. The Time Correlated Single Photon Counting (**TCSPC**) measurements were carried out using IBH picoseconds single photon counting machine. The sample is excited with a pulsed diode laser at a wavelength of 480 nm (Nano-LED) with a repletion of 100 kHz. The pH of various samples were analysed using Cyberscan Eutech pH meter (Ruosull Technology Co., China).

Synthesis of red fluorescent gold nanoclusters (Au–BSA NCs). The preparation was performed

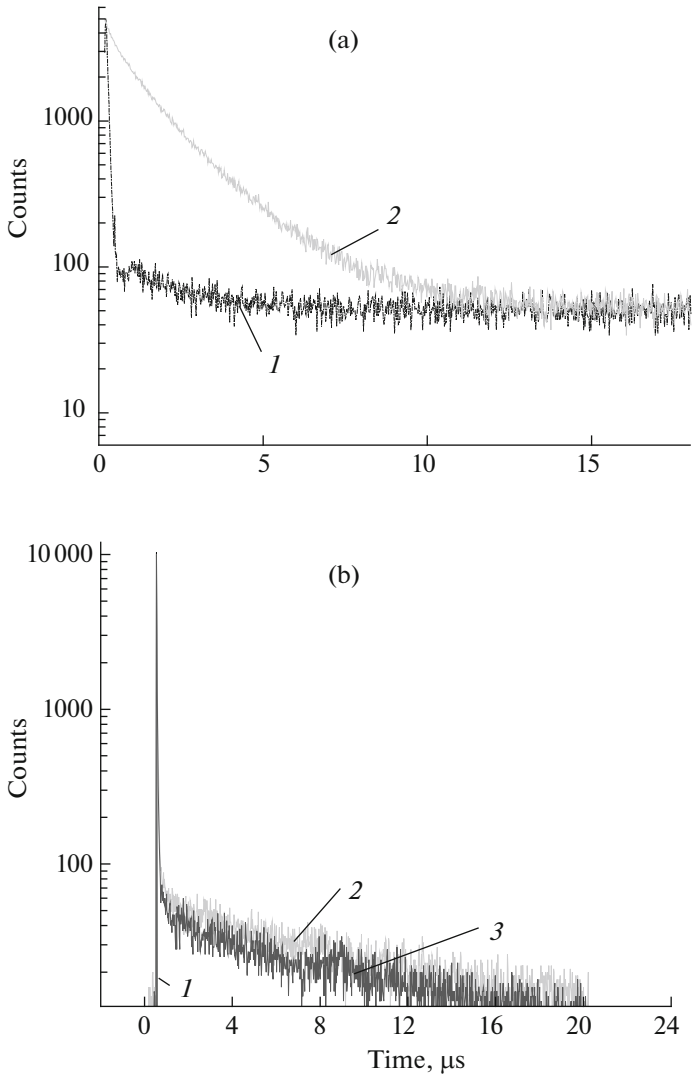

Fig. 3. (a) Fluorescence lifetime decay curves of Au–BSA NCs, prompt (*1*) and decay (*2*) curves. (b) Fluorescence lifetime decay curve of boronic acid conjugated gold nanoclusters and lactose quenched boronic acid conjugated gold nanoclusters: prompt (*1*) and decay (*2*) curves of boronic acid conjugated gold nanoclusters; decay curve of lactose quenched boronic acid conjugated gold nanocluster (*3*).

according to the previously reported method with slight modifications [4]. Typically, 15.00 mL of 10 mM $HAuCl_4$ solution was added to 15.00 mL of 50 mg/mL BSA solution under vigorous stirring at physiological temperature, 37°C. Two minutes later 1.50 mL of 1.0 M NaOH solution was introduced (pH ~ 12) and the mixture was stirred vigorously at 37°C for 12 h. The colour of the solution changed from light yellow to light brown and then to characteristic dark brown of AuNCs. The as-prepared solution was then dialysed in double distilled water for 48 h to get refined product. Finally the obtained AuNCs solution was stored at 4°C for further use.

Synthesis of Au–BSA–APBA probe. (3-Aminophenyl)boronic acid **(**APBA) was immobilised on to Au–BSA NCs by using coupling agents (EDC and NHS). Typically 5.00 mL of Au–BSA NCs solution was diluted to 10.00 mL with distilled water. Then 57.5 mg EDC was added to 10.00 mL of this Au–NCs solution and stirred in dark for 10 min after which 34.5 mg of NHS was poured into the mixture under the same experimental condition. After 2 h reaction at room temperature with stirring in dark, 75.0 mg APBA was added in to the activated Au–BSA NCs solution and the new system was incubated for 12 h. The as-prepared Au–BSA–APBA probe was separated from impurities using ultracentrifugation (75000 rpm,

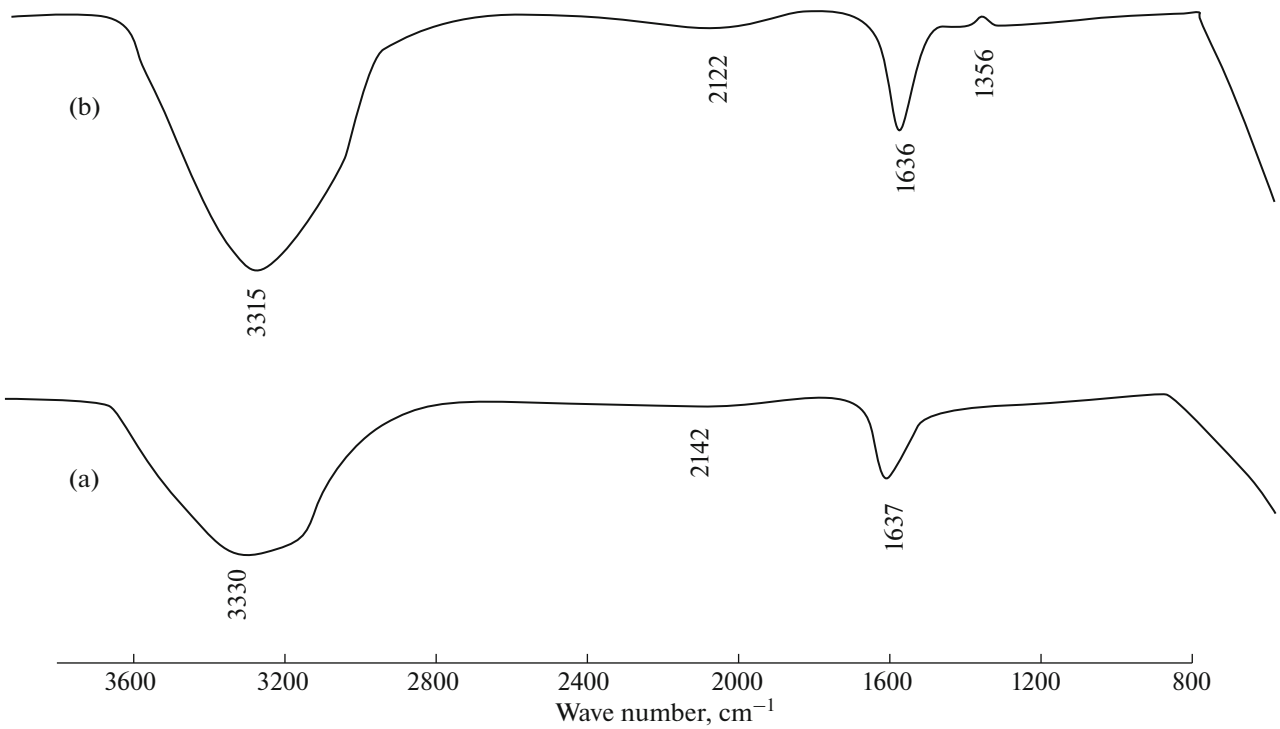

Fig. 4. FT-IR spectra of Au–BSA NCs (a) and Au–BSA–APBA probe (b).

30 min) to get purified product. Then the Au–BSA–APBA probe solution is diluted to 40.00 mL and used for further characterization.

Synthesis of Au–BSA–APBA–lactose conjugate. Typically, 200 μL of 0.01 M lactose solution was added to 3.00 mL Au–BSA–APBA probe solution and incubated for 30 min at room temperature for further characterization.

RESULTS AND DISCUSSION

Synthesis and characterisation of AuNCs and Au–BSA–APBA probe. The gold nanoclusters were synthesised through a protein directed green process where bovine serum albumin acted both as reducing and capping agent. In contrast to the oxidation of neutral gold in highly acidic aqua-regia, Au(III) ion of the added gold chloride get reduced to Au(I) at high basic pH of 12. The final reduction of Au(I) to Au(0) is carried out by aromatic tyrosine residue present in BSA. The disulphide bonds which hide inside the secondary structure of protein at low pH became available for strong Au–S bonds at pH 12 and provide appreciable capping ability for protein. The steric effects due to largeness of protein also have a role in stabilization of AuNCs by BSA [4].

The formation of Au–BSA NCs was first found by the colour change from yellow to dark brown in visible light (Fig. 1a). The fluorescence spectrum of AuNCs with excitation at 480 nm showed emission maximum at 622 nm as evident from Fig. 1b.

The size distribution of AuNCs prepared was determined using dynamic light scattering (**DLS**) and recorded as 4.3 nm, as shown in Fig. 2a. This is the hydrodynamic diameter, and the actual size of cluster will meet the sub-nanometer size of fluorescent gold nanocluster. Thus DLS data can be considered as a proof for successful synthesis of ultrasmall AuNCs.

To evaluate the fluorescent emission from gold nanocluster, we measured fluorescence life-time of Au–BSA NCs prepared in our lab using TCSPC. Figure 3 presents the fluorescence decay curves from Au–BSA NCs which got fit in bi-exponential model to obtain one long and one short lifetime components. The decay process was dominated by slow component in microsecond time scale i.e., 1.81 μs (80%). The other fast component is 560.3 ns (20%). The average lifetime of gold nanocluster was calculated to be 1.72 μs. The systematic examination of lifetime of various thiol or protein-protected gold nanoclusters showed either single exponential or biexponential decay curves [52, 53]. Moreover, the values for lifetime component also varies. This disparity in reports implies the probable dependence of fluorescence lifetime decay on the nature of ligand as well as the experimental conditions of synthesis (for example, pH). Fortuitously, the photo-carrier (excited electron) in Au_{25} nanoclusters mostly follows bi-exponential decay

[52, 54]. This bi-exponential fit is correlated to the spectral overlap between dominated thermally activated delayed fluorescence in microsecond time scale and prompt fluorescence in nanosecond time scale in red fluorescence of BSA-protected Au_{25} nanoclusters [54]. Thus, bi-exponential fit of our gold nanoclusters further prove the existence of Au_{25} entity in our biosensor [54].

The as-prepared gold nanoclusters contain groups of gold atoms in nanometer dimension trapped inside the folding of BSA protein [4]. There were several free carboxylic and amino groups on the surface of Au–BSA NCs. The presence of the free carboxylic groups on surface of NCs provides an opportunity to bind it with 3-aminophenylboronic acid through EDC coupling chemistry (Scheme 1):

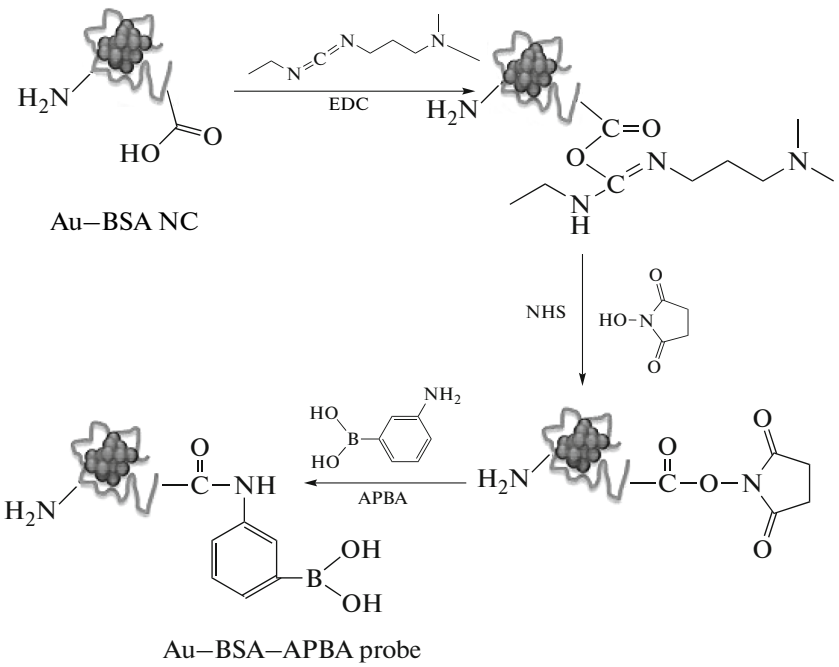

Scheme 1. Formation of boronic acid conjugated gold nanoclusters (Au–BSA–APBA probe) through carbodiimide (EDC) coupling chemistry.

FT-IR spectral studies were carried out to account for the surface functionalization of AuNCs with APBA (Fig. 4). While comparing the FT-IR spectra of Au–BSA NCs and Au–BSA–APBA probe, the Gaussian peak corresponding to O–H stretching of AuNCs was slightly shifted to 3315 cm^{-1} denoting the merging of O–H and N–H stretching vibration into a single peak upon APBA conjugation. The strong B–O stretching band appeared as a shoulder peak at 1356 cm^{-1} in Au–BSA–APBA probe to confirm the surface functionalization of AuNCs with boronic acid.

The surface modification of AuNCs on probe fabrication can be further inferred from the blue shift observed in the fluorescence spectrum of Au–BSA–APBA probe (Fig. 1b). On the formation of Au–BSA–APBA probe, fluorescence enhanced by 73% as compared to AuNCs from which it was synthesised. This rise in fluorescence intensity of Au–BSA–APBA probe can be substantiated by the fact that APBA immobilisation introduces an electron-rich nitrogen atom on the cluster surface. The fluorescence of newly formed probe gets improved with the increased direct donation of delocalised electrons of the ligand to the metal core of AuNCs via surface interaction [53].

Fluorescence quenching of Au–BSA–APBA probe by saccharides. Boronic acid functionalised probe can react with 1,2- or 1,3-*cis*-diols in polyols like saccharides. As shown in Scheme 2, a reversible equilibrium exists between boronic acid and boronate ester on the interaction of boronic acids and *cis*-diol of saccharides. The ester formation is favourable in solutions of high pH in which the boronate ion exist in high concentration. It is reported [39] that the formation of

tetra-coordinated hydroxyboronate complexes of 1,2-diols at high pH is accompanied by a significant release of angle strain resulting from the rehybridisation of the boron from sp^2 to sp^3.

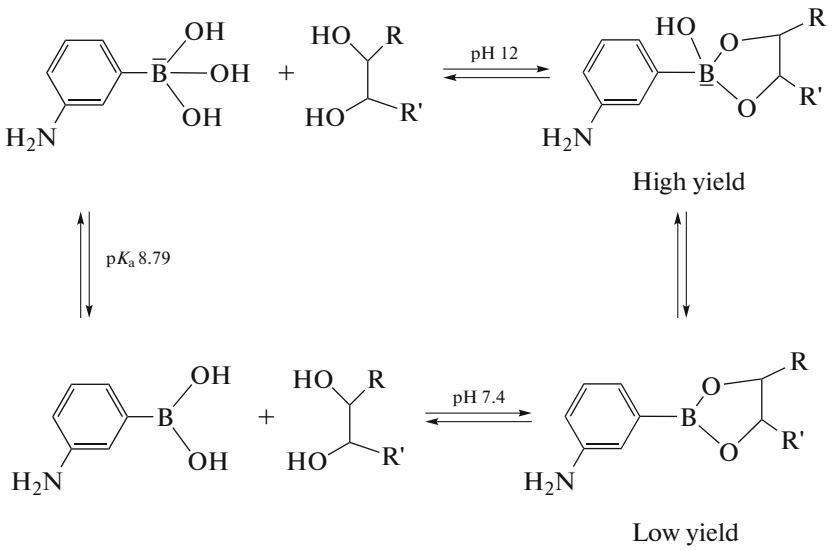

Scheme 2. Equilibrium formation of boronate esters from diols at high pH (12) and physiological pH (7.4).

We investigated the fluorescence response of Au–BSA–APBA probe by different saccharides like glucose, lactose and galactose under optimal conditions (pH 12, room temperature, 30 min incubation). Interestingly we found that lactose exhibit highest sensitivity towards Au–BSA–APBA probe than glucose and galactose (Fig. 5). The specific response of lactose towards the turn-off sensor can be attributed to the effective boronate ester formation of lactose with boronic acid part of more than one sensor entity at a time using two sets of *cis*-diol groups in lactose molecule. In contrast, other mono-saccharides tested here possess single set of 1,2-*cis*-diols in their structure although they can form boronate ester. The structures of these saccharides are shown as Scheme 3. As shown in Fig. 5c, the fluorescence intensity of Au–BSA–APBA probe decreased gradually with a slight blue shift as the concentration of lactose increased. The limit of detection of this probe towards lactose was observed as 0.02 μM.

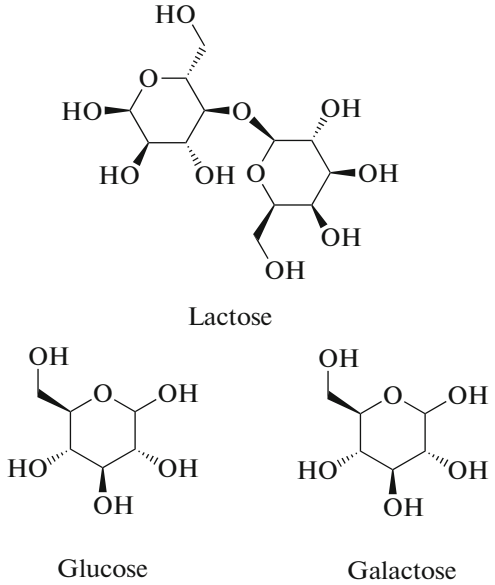

Scheme 3. Structures of lactose, glucose and galactose.

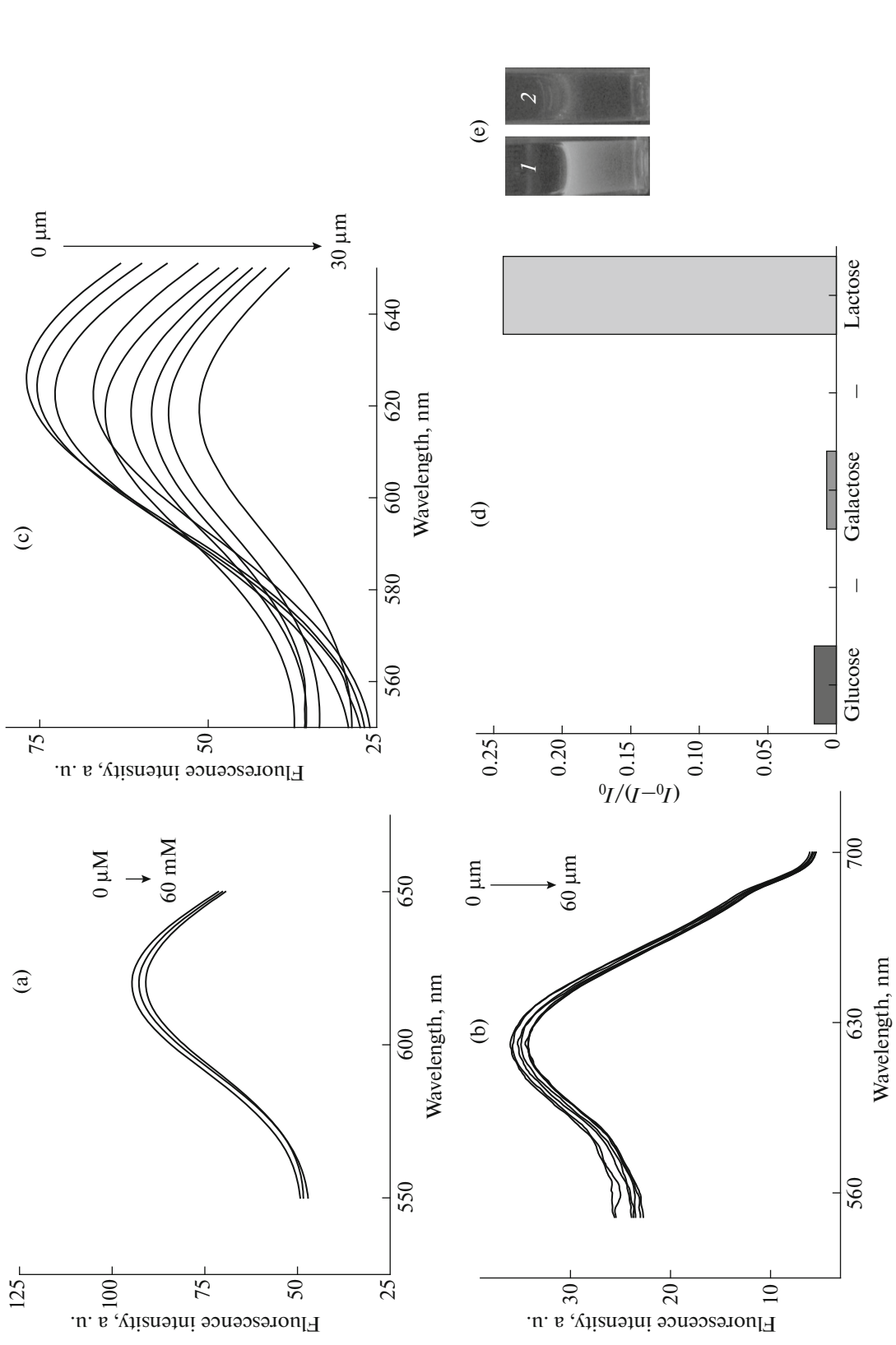

Fig. 5. (a) The fluorescence response of the Au–BSA–APBA probe upon addition of various concentrations of glucose at a pH 12 (from top: 0, 2, 5, 10, 20, 30, 60 μM); (b) the fluorescence response of the Au–BSA–APBA probe upon addition of various concentrations of galactose at a pH of 12 (from top: 0, 2, 5, 10, 20, 30, 60 μM); (c) the fluorescence response of the Au–BSA–APBA probe upon addition of various concentrations of lactose at pH 12 (from top: 0, 2, 5, 7, 10, 15, 20, 25, 30 μM); (d) selectivity of the Au–BSA–APBA probe for lactose over other saccharides at pH 12; (e) photographs of the Au–BSA–APBA conjugate before (*1*) and after (*2*) the addition of lactose under UV light illumination.

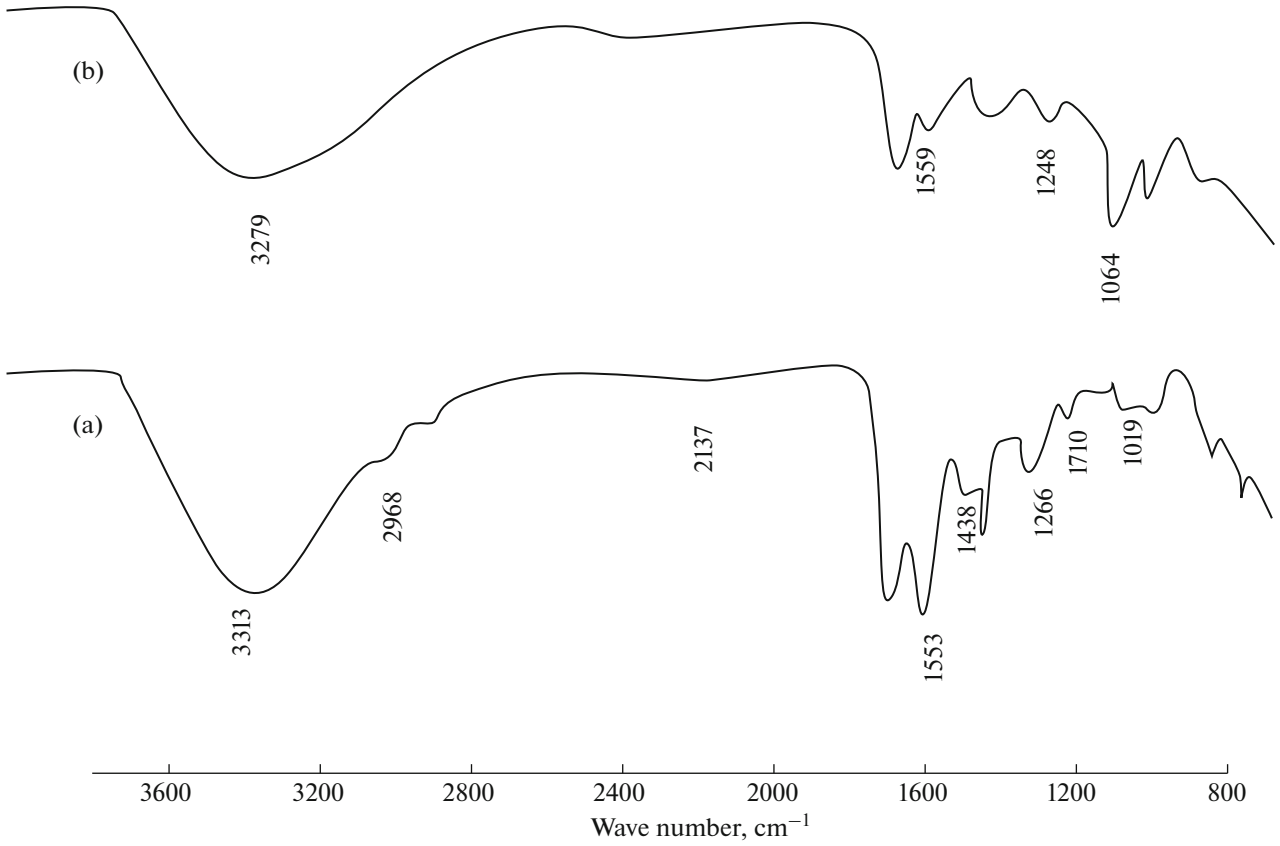

Fig. 6. The FT-IR spectrum of Au–BSA–APBA–lactose conjugate (a) and Au–BSA–APBA–lactose–dopamine system (b).

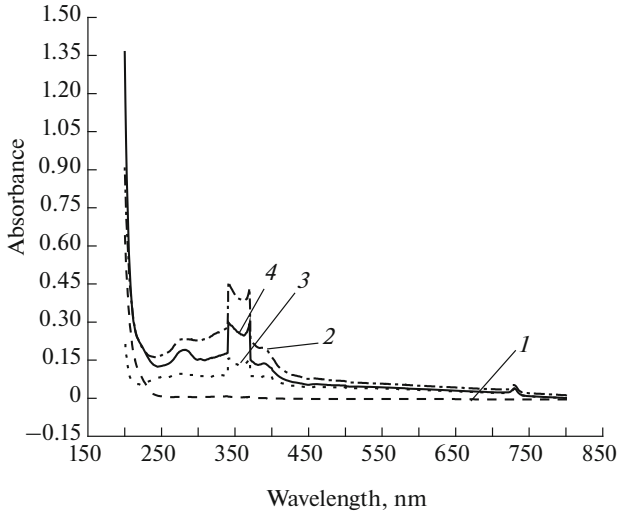

Fig. 7. The UV-visible absorption spectra of gold nanoclusters prepared using BSA-directed synthesis, Au–BSA NCs (*1*); boronic acid conjugated gold nanoclusters, Au–BSA–APBA probe (*2*); lactose tailored boronic acid conjugated gold nanocluster, Au–BSA–APBA–lactose conjugate (*3*); dopamine added lactose tailored boronic acid conjugated gold nanoclusters (*4*).

Moreover, the formation of Au–BSA–APBA–lactose conjugate was further verified by IR spectral studies (Fig. 6). The peaks assigned to C–O stretching of esters (1266 and 1170 cm^{-1}) confirmed the conjugate formation with lactose. Also, the optical property in each stage of sensor design is analysed using UV-Vis spectroscopy (Fig. 7).

The Stern–Volmer plot was constructed to determine the relationship between the quenching effect (I_o/I) on Au–BSA–APBA probe with the different concentration of quencher molecules. The fitted linear data could be expressed as: (I_o/I) = 1.00799 + 0.01587[lactose]; R^2 = 0.986. The Stern–Volmer quenching constant was obtained as 0.01587 μM^{-1}. The linear nature of Stern–Volmer plot indicates either pure static or pure dynamic type of quenching [55]. The DLS data shows a size increase (54.7 nm) upon Au–BSA–APBA–lactose conjugate formation (Fig. 2b) and support the possibility of aggregation induced static quenching where a fluorophore forms a non-fluorescent complex in its ground state [55]. In presence of lactose, boronate ester is formed between boronic acid part of probe and saccharide in solution. Consequently

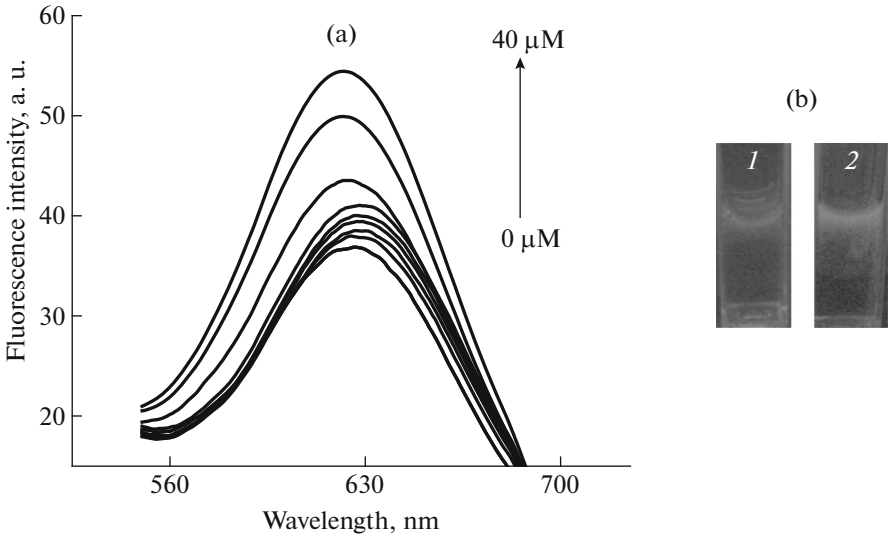

Fig. 8. (a) The fluorescence response of the Au–BSA–APBA–lactose conjugate upon addition of various concentrations of dopamine at pH 12 (from bottom: 0, 2, 5, 7, 10, 15, 20, 30, 40 μM); the concentration of lactose is 10 mM. (b) The photographs of Au–BSA–APBA–lactose conjugate (*1*) and Au–BSA–APBA–lactose–dopamine system (*2*) under UV irradiation.

one sugar moiety interacts with more than one Au–BSA–APBA probe resulting in the aggregation leading to quenching of fluorescent probe. The whole mechanism is represented in Scheme 4.

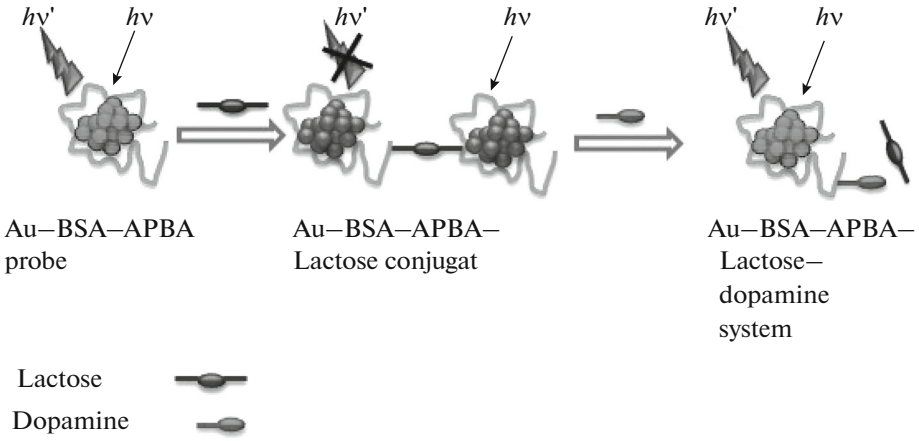

Scheme 4. Schematic illustration of mechanism for detection of dopamine with lactose tailored boronic acid conjugated gold nanocluster.

"Turn-on" sensing of dopamine with Au–BSA–APBA–lactose conjugate. With the addition of series of concentration of dopamine, the fluorescence of system enhanced with a small blue shift as shown in Fig. 8a. This can be attributed to the displacement of lactose by dopamine, thereby rupturing the aggregates and recovering the fluorescence. The fluorescence intensity increased linearly with the concentration of dopamine. The blue shift in the fluorescence is an indicator of surface modification of AuNCs on ester formation. A dose-response graph was constructed to examine the relationship between the degree of fluorescence enhancement of the turn-on sensor and the concentration of the analyte, that is the dependence of fluorescence enhancement (ΔF) on the concentration of dopamine. The fitted linear data could be expressed as $\Delta F = 0.43718$[dopamine] $- 0.69148$, $R^2 = 0.97004$. The limit of detection for dopamine was 0.7 μM.

Dopamine, with its limited number of OH-groups, could interact with only one Au–BSA–APBA probe to form a stable complex. Hence dopamine prevents the aggregation and retained the fluorescence of the system as described in Scheme 4. Moreover dopamine offers an internal coordination between the nitrogen

Table 2. Determination of dopamine in blood serum and urine by the proposed method

Sample	Added, μM	Found, μM	Recovery, %
Serum 1	20	20.4 ± 0.14	101.2 ± 0.7
Serum 2	30	30.5 ± 0.1	101.7 ± 0.2
Urine 1	20	20.5 ± 0.1	102.3 ± 0.4
Urine 2	30	30.7 ± 0.1	102.3 ± 0.4

lone pair and boron's vacant orbital during the tetrahedral complex formation. This coordination makes the backward reaction less favourable and eventually stabilises the B atom [39]. The rapid response of our sensor proves the extra stability of boronate ester with dopamine as compared to lactose–boronic acid complex.

In order to confirm the idea about mechanism of turn-on sensing, we characterised the Au–BSA–APBA–lactose–dopamine system using FT-IR (Fig. 8). The =C–O stretching of ester at 1248 cm^{-1} confirmed the boronate ester formation with dopamine. As an indicator of change of functionalization on ligand, a new band appeared at 1064 cm^{-1} that can be assigned to C–N stretching of amides.

Selectivity. Initially we investigated the fluorescence response of Au–BSA–APBA–lactose conjugate in the presence of other catechol amines (Scheme 5) such as adrenaline and noradrenaline. To our delight, the proposed nano-sensor was specific for dopamine with respect to the other catechol amines as shown in Fig. 9a. This selectivity can be ascertained to the extra-stability of dopamine–boronic acid complex by the internal coordination between the nitrogen lone pair and boron's vacant *p* orbital [39]. This internal conjugation is not so effective in other analogues where bulky substituent such as –OH and $-CH_3$ provide steric barriers.

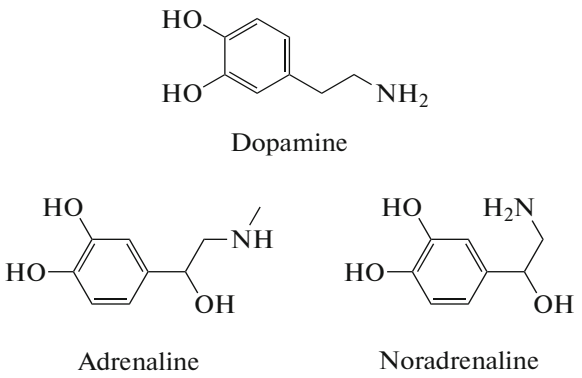

Scheme 5. The structures of catecholamines.

Furthermore, we studied the influence of other possible coexisting interfering substances over dopamine detection. The fluorescence response of the Au–BSA–APBA–lactose conjugate with five other bioanalytes including ascorbic acid, uric acid, arginine, histidine and lysine were shown in Fig. 9b. Among the possible interfering biological species, ascorbic acid presented notable response of the sensor. This interfering effect can be attributed to the probable 1,2-*cis*-diol-boronic acid interaction between hydroxide groups of ascorbic acid and boronic acid part of the turn-on sensor. However it was interesting to note that the sensitivity of dopamine remain immune to the combined influence of five interfering analytes present as a mixture along with dopamine. This selectivity could also support the extra-stability of dopamine complex with boronic acid conjugate.

Application. The specificity and sensitivity of Au–BSA–APBA–lactose conjugate to dopamine proposed that our method might be directly applied for detecting dopamine in real samples. To evaluate whether the turn-on green sensor is applicable to natural system, determination of dopamine in spiked human blood serum and urine samples were conducted. The real samples were diluted to 10 times with distilled water before measurement. No other pretreatment was performed. Thus the proposed system gave rise to excellent recoveries in spiked real samples. The analytical results were shown in Fig. 10 and listed in Table 2. The low relative standard deviations (**RSD**s) prove the accuracy and reliability of the proposed method. Since less than 1 min was required to run a single assay, this approach appears to be suitable for the rapid and simple analysis.

CONCLUSIONS

In summary, we have demonstrated lactose tailored boronic acid conjugated gold nanoclusters as an excellent platform for fluorescence turn-on sensing of dopamine in aqueous solution with high sensitivity and selectivity. In the preliminary stage of investigation, we found that the fluorescence of Au–BSA–APBA probe can be switched off effectively by lactose through aggregation-induced quenching. Thus the initial probe can be used for detection of lactose. The resulting Au–BSA–APBA–lactose conjugate was further employed for turn-on sensing of dopamine. This turn-on sensor is selective for dopamine over other catechol amines as well as other bioanalytes including coexisting biomolecules. The real sample analysis of dopamine in blood serum and urine samples was performed and found good. Therefore newly synthesised Au–BSA–APBA probe can be used as a *green* dual mode turn-off – turn-on nano-sensor. This simple method without a tedious and time-consuming procedure would expect to have fruitful application in detection of dopamine in future medical diagnosis and therapeutics.

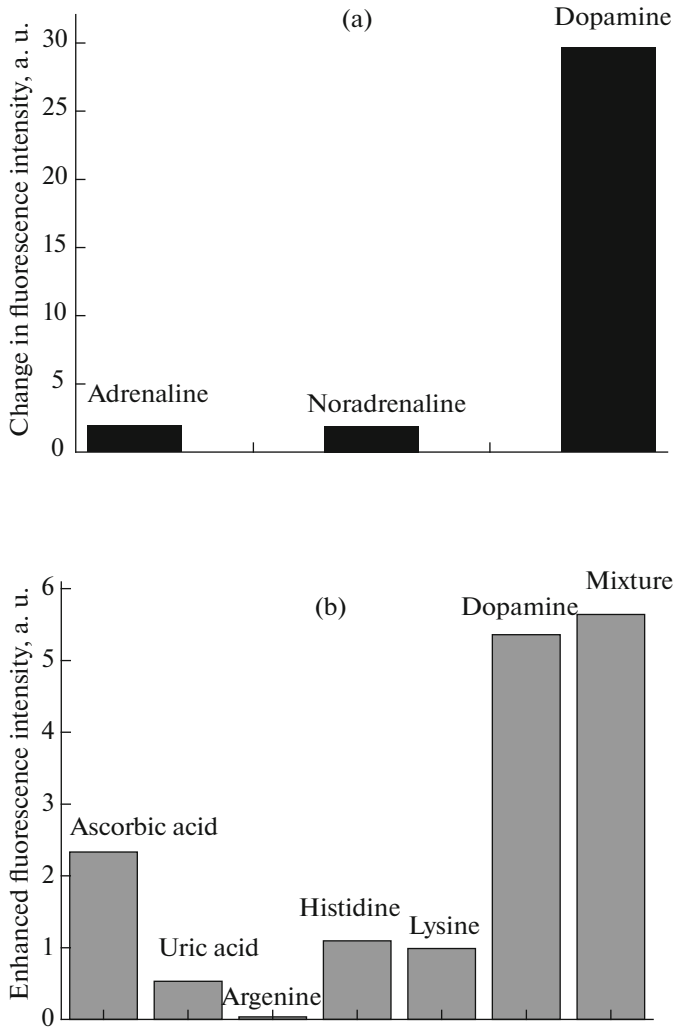

Fig. 9. Signal of Au–BSA–APBA–lactose conjugate in the presence of other catecholamines (a) and interfering bioanalytes (b).

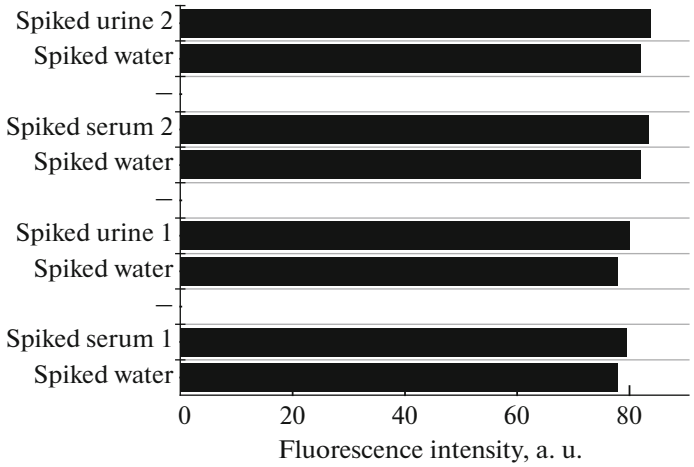

Fig. 10. Fluorescence response of the Au–BSA–APBA–lactose conjugate of different real samples and distilled water samples spiked with dopamine at pH 12.

ACKNOWLEDGMENTS

The authors thank SCT IMST, Trivandrum for facilitating the TEM analysis and Department of Chemistry, Kariavattom for providing the instrumental facilities and support. The authors are grateful to Dr. Meena T. Pillai (Professor, University of Kerala) for her efforts in improving the language of this manuscript.

REFERENCES

1. Oliver-Meseguer, J., Cabrero-Antonino, J.R., Dominguez, I., Leyva-Perez, A., and Corma, A., *Science*, 2012, vol. 338, p. 1452.
2. Yoon, B., Hakkinen, H., Landman, U., Worz, A.S., Antonietti, J.-M., Abbet, S., Judai, K., and Heiz, U., *Science*, 2005, vol. 307, p. 403.
3. Qian, H., Zhu, M., Wu, Z., and Jin, R., *Acc. Chem. Res.*, 2012, vol. 45, p. 1470.
4. Xie, J., Zheng, Y., and Ying, J.Y., *J. Am. Chem. Soc.*, 2009, vol. 131, p. 888.
5. Lin, C.J., Lee, C.H., Hsieh, J., Wang, H., Li, J.K., She, J., Chan, W., Yeh, H., and Chang, W.H., *J. Med. Biol. Eng.*, 2009, vol. 29, no. 6, p. 276.
6. Zheng, J., Zhang, V., and Dickson, R.M., *Phys. Rev. Lett.*, 2004, vol. 93, 0774021.
7. Ho, J.A., Chang, H., and Su, V., *Anal. Chem.*, 2012, vol. 84, p. 3246.
8. Zhang, G., Li, Y., Xu, J., Zhang, V., Shuang, S., Dong, C., and Choi, M.M.F., *Sens. Actuators B*, 2013, vol. 183, p. 583.
9. Palmal, S., Basiruddin, S.K., Maity, A.R., Ray, S.C., and Jana, N.R., *Chem. Eur. J.*, 2013, vol. 19, p. 943.
10. Dou, Y. and Yang, X., *Anal. Chim. Acta*, 2013, vol. 784, p. 53.
11. Kennedy, T.A.C., MacLean, J.L., and Liu, J., *Chem. Commun.*, 2012, vol. 48, p. 6845.
12. Bao, Y., Zhong, C., Vu, D.M., Temirov, J.P., Dyer, R.B., and Martinez, J.S., *J. Phys. Chem. C*, 2007, vol. 111, p. 12194.
13. Mu, X., Qi, L., Dong, P., Qiao, J., Hou, J., Nie, Z., and Ma, H., *Biosens. Bioelectron.*, 2013, vol. 49, p. 249.
14. Yu, P., Wen, X., Toh, Y., and Tang, J., *J. Phys. Chem. C*, 2012, vol. 116, p. 6567.
15. Wei, H., Wang, Z., Yang, L., Tian, S., Hou, C., and Lu, Y., *Analyst*, 2010, vol. 135, p. 1406.
16. Wang, Y., Chen, J., and Yan, X., *Anal. Chem.*, 2013, vol. 85, p. 2529.
17. Garcia, A.R., Rahn, I., Johnson, S., Patel, R., Guo, J., Orbulescu, J., Micic, M., Whyte, J.D., Blackwelderd, P., and Leblan, R.M., *Colloids Surf. B*, 2013, vol. 105, p. 167.
18. Xia, X., Long, Y., and Wang, J., *Anal. Chim. Acta*, 2013, vol. 772, p. 81.
19. Park, K.S., Kim, M.I., Woo, M., and Park, H.G., *Biosens. Bioelectron.*, 2013, vol. 45, p. 65.
20. Liu, Y., Ai, K., Cheng, X., Huo, L., and Lu, L., *Adv. Funct. Mater.*, 2010, vol. 20, p. 951.
21. Liu, H., Yang, G., Abdel-Halim, E.S., and Zhu, J., *Talanta*, 2013, vol. 104, p. 135.
22. Cai, Y., Yan, L., Liu, G., Yuan, H., and Xiao, D., *Biosens. Bioelectron.*, 2013, vol. 41, p. 875.
23. Zhang, M., Dang, Y., Liu, T., Li, H., Wu, Y., Li, Q., Wang, K., and Zou, B., *J. Phys. Chem. C,* 2013, vol. 117, p. 639.
24. Durgadas, C.V., Sharma, C.P., and Sreenivasan, K., *Analyst*, 2011, vol. 136, p. 933.
25. Lin, Z., Luo, F., Dong, T., Zheng, L., Wang, Y., Chi, Y., and Chen, G., *Analyst*, 2012, vol. 137, p. 2394.
26. Chen, Z., Zhang, G., Chen, X., Chen, J., Liu, J., and Yuan, H., *Biosens. Bioelectron.*, 2013, vol. 41, p. 844.
27. Wen, F., Dong, Y., Feng, L., Wang, S., Zhang, S., and Zhang, X., *Anal. Chem.*, 2011, vol. 83, p. 1193.
28. Peng, J., Feng, L., Zhang, K., Li, X., Jiang, L., and Zhu, J., *Chem. Eur. J.*, 2012, vol. 18, p. 5261.
29. Wang, J., Zhang, G., Li, Q., Jiang, H., Liu, C., Amatore, C., and Wang, X., *Sci. Rep.*, 2013, vol. 3, p. 115.
30. Lin, C.J., Chuang, W., Huang, Z., Kang, S., Chang, C., Chen, V., Li, J., Li, J.K., Wang, H., Kung, F., Shen, J., Chan, W., Yeh, C., Yeh, H., Lai, W.T., and Chang, W.H., *ACS Nano*, 2012, vol. 6, p. 5111.
31. Wang, Y., Chen, J., and Irudayaraj, J., *ACS Nano*, 2011, vol. 5, p. 9718.
32. Imahori, H. and Fukuzumi, S., *Adv. Mater.*, 2001, vol. 13, p. 1197.
33. Su, L., Shu, T., Wanga, Z., Cheng, J., Xue, F., Li, C., and Zhang, X., *Biosens. Bioelectron.*, 2013, vol. 44, p. 16.
34. Huang, X., Luo, Y., Li, Z., Li, B., Zhang, H., Li, L., Majeed, I., Zou, P., and Tan, B., *J. Phys. Chem. C*, 2011, vol. 115, p. 16753.
35. Wang, H., Lin, C.J., Lee, C., Lin, Y., Tseng, Y., Hsieh, C., Chen, C., Tsai, C., Hsieh, C., Shen, J., Chan, W., Chang, W.H., and Yeh, H., *ACS Nano*, 2011, vol. 5, p. 4337.
36. Lin, C.J., Yang, T., Lee, C., Huang, S.H., Sperling, R.A., Zanella, M., Li, J.K., Shen, J., Wang, H., Yeh, H., Parak, W.J., and Chang, W.H., *ACS Nano*, 2009, vol. 3, p. 395.
37. Hu, L., Hana, S., Parveen, S., Yuana, Y., Zhang, L., and Xu, G., *Biosens. Bioelectron.*, 2012, vol. 32, p. 297.
38. Chen, Z., Qian, S., Chen, J., and Chen, X., *J. Nanopart. Res.*, 2012, vol. 14, p. 1264.
39. Hall, D.G., *Boronic Acids: Preparation, Applications in Organic Synthesis and Medicine*, Weinheim: Wiley, 2005.
40. Zhang, W., He, X., Yang, Y., Li, W., and Zhang, Y., *J. Mater. Chem. B*, 2013, vol. 1, p. 347.
41. Zhang, X., Wu, Y., Tu, Y., and Liu, S., *Analyst*, 2008, vol. 133, p. 485.
42. Li, Y., Hong, M., Miaomiao, Bin, Q., Lin, Z., Cai, Z., and Chen, G., *J. Mater. Chem. B*, 2013, vol. 1, p. 1044.
43. Damier, P., Hirsch, E.C., Agid, Y., and Graybiel, A.M., *Brain*, 1999, vol. 122, p. 1437.
44. Zhang, A., Neumeyer, J.L., and Baldessarini, R.J., *Chem. Rev.*, 2007, vol. 107, p. 274.

45. Downard, A.J., Roddick, A.D., and Bond, A.M., *Anal. Chim. Acta*, 1995, vol. 317, p. 303.

46. Ping, J., Wu, J., Wang, Y., and Ying, Y., *Biosens. Bioelectron.*, 2012, vol. 34, p. 70.

47. Tsai, T., Huang, F., and Chen, J.J., *Sens. Actuators B*, 2013, vol. 181, p. 179.

48. Carrera, V., Sabater, E., Vilanova, E., and Sogorb, M.A., *J. Chromatogr. B*, 2007, vol. 847, p. 88.

49. Ma, Y., Yang, C., Li, N., and Yang, X., *Talanta*, 2005, vol. 67, p. 979.

50. Germain, M.E. and Knapp, M.J., *Chem. Soc. Rev.*, 2009, vol. 38, p. 2543.

51. Jun, M.E., Roy, B., and Ahn, K.H., *Chem. Commun.*, 2011, vol. 47, p. 7583.

52. Guevel, X.L., Hotzer, B., Jung, G., Hollemeyer, K., Trouillet, V., and Schneider, M., *J. Phys. Chem. C*, 2011, vol. 115, p. 10955.

53. Wu, Z. and Jin, R., *Nano Lett.*, 2010, vol. 10, p. 2568.

54. Wen, X., Yu, P., Toh, Y., Hsu, A., Lee, Y., and Tang, J., *J. Phys. Chem. C*, 2012, vol. 116, p. 19032.

55. Lakowicz, J.R., *Principles of Fluorescence Spectroscopy*, New York: Springer, 2006.